

Model of a Solar Collector/Storage System for Industrial Thermal Applications*

A. Baldini, G. Manfrida^{1**}, D. Tempesti
Università degli Studi di Firenze, Dipartimento di Energetica "Sergio Stecco"
via C. Lombroso 6/17, Florence, Italy,
Email: ¹Manfrida@unifi.it

Abstract

A model for the thermodynamic analysis of a non-stationary solar thermal system is described. The main system components are a parabolic tube collector and a steam accumulator, which provides heat for industrial processes. The use of exergy analysis leads to the identification of potentials for performance improvements. The rate of exergy destruction is calculated over a daily operation cycle, showing that the largest exergy destruction takes place at collector level. The effect of varying the volumetric flow rate per unit collector surface area is also discussed.

Keywords: Solar energy, thermal storage, industrial energy processes, exergy analysis.

1. Introduction

Solar farms using focusing thermal collectors in combination with a steam turbine system represent a proven energy conversion technology which is competitive with photovoltaic for electricity production (Mills, 2004). This advantage is even greater if combined heat and power production is considered.

The production of heat for industrial processes is much less common when the sun is considered as the primary energy source. This option should be considered with more attention, however, because the equipment can be much simpler than in the case of electricity production (see International Energy Agency Task 33 Solar Heating and Cooling, www.iea-shc.org/task33). The use of solar energy for heat supply in the industrial sector, e.g. in food processing and in textile industries, has the potential for a substantial economization of primary energy resources. Another advantage would be an improved public perception of the product and the company. Process heat can usually be provided at much lower temperatures and pressures than those necessary for electricity production. Simpler concentrating collectors can be used and the cost of equipment is much smaller. A key issue is matching the exergy of the source (the sun) and the heat demands of the industrial processes. Therefore, a heat storage system is generally required. Since heat in industrial applications is usually provided by saturated steam, one of the most popular options is moderately pressurized water (5-30 bar). If the storage tank is correctly sized, the necessary process steam can be supplied by depressurization.

2. Model of the System

A simplified layout of the solar collector system with process steam production is shown in Figure 1. One of the system boundaries is the solar collector, where in a primary circuit a high-temperature heat transfer fluid in liquid phase absorbs the heat from solar radiation.

The collector is modeled by the Bliss equation (Duffie and Beckman, 2006):

$$\eta_{coll} = A - B \cdot X - C \cdot I \cdot X^2 \quad (1)$$

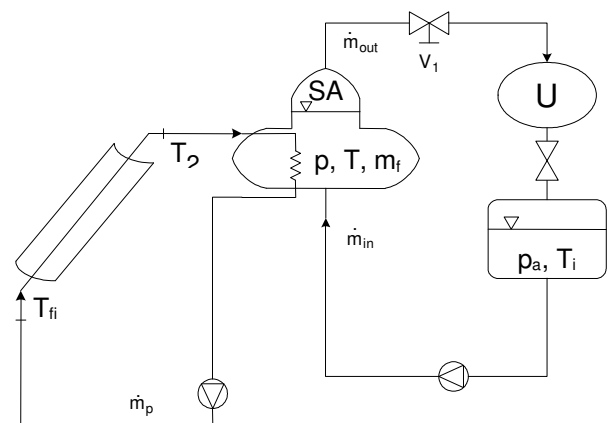


Figure 1: Schematic Diagram of the System.

with

$$X = [(T_{fo} + T_{fi})/2 - T_a]/I \quad (2)$$

Constants A, B and C can either be determined experimentally or calculated considering the optical and heat transfer losses of the collector (Winter, 1991). In this paper the operating data for a Solartech[®] concentrating parabolic collector are used. The efficiency curve of this collector is shown in Figure 2. The amount of solar radiation on the mirror surface is given by the following equation (Duffie and Beckman, 2006):

$$Hb_{tracking} = \frac{\cos(\theta)}{\cos(\theta_z)} \cdot Hb_{horizontal} \quad (3)$$

with

$$\cos(\theta) = \sqrt{\cos^2(\theta_z) + \cos^2(\delta) + \sin^2(\omega)} \quad (4)$$

*This paper is an updated version of a paper published in the ECOS08 proceedings. It is printed here with permission of the authors and organizers.

**Corresponding Author

Although the heat transfer fluid here considered is pressurized water, any single-phase fluid for high-temperature heat transfer can be used (Camacho et al, 1997). Recent options include partially ionized fluids and molten salts (ENEA-Archimede Project Grande Progetto Solare Termodinamico, www.enea.it/com/solar), however these require a back-up heating system to maintain the salts in a liquid state.

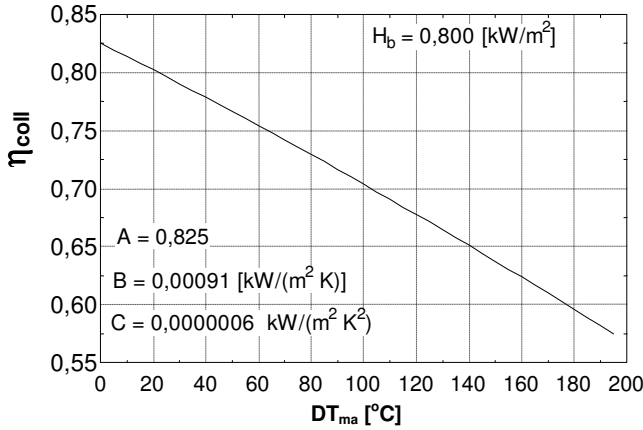


Figure 2: Solartech® Collector Efficiency.

The secondary circuit receives heat from the primary circuit. The fluid of the secondary circuit is stored in a steam accumulator (SA), which we modeled as a perfectly-stirred adiabatic system that operates between two limiting liquid levels (full/empty) with a liquid/vapor separation interface. Saturated steam is taken at a rate \dot{m}_{out} from the top of the SA and supplied to the thermal user U (see Figure 1). Water leaving the condensate recovery tank of the production plant enters the bottom of the SA with a flow rate of \dot{m}_{in} at sub-cooled conditions.

When the user's heat demand increases, the steam valve V_1 is opened to increase the steam flow rate. Consequently, the SA is de-pressurized, and flash steam is produced. During this transient period, the level in the SA is falling. In order to prevent this level from falling below the lower limit, the condensate flow rate has to be increased, or the solar collector has to provide more heat. The latter, of course, depends on weather conditions. If, on the other hand, no heat is extracted from the SA ($\dot{m}_{out} = 0$), the continuous heat input from the solar collector and the condensate inlet flow rate ($\dot{m}_{in} \neq 0$) leads to a rise in the SA filling level. The model not only include limits for the SA filling level, but also limits for the SA operating pressures that are consistent with common specifications for steam production.

Assuming that all fluid mass is stored in the liquid phase due to its much higher density, the mass variation in the SA is equivalent to the average mass flow rate due to phase transition (flashing). The mass balance of the SA can then be written as:

$$\dot{m}_{PT} = \frac{dM}{dt} = \dot{m}_{out} - \dot{m}_{in} \quad (5)$$

Under the assumption of no thermal stratification, the energy balance for the dynamic model of the SA can be written as:

$$\frac{dU}{dt} = \dot{m}_{in} \cdot h_{in} - \dot{m}_{out} \cdot h_{out} + \dot{Q}_{coll} \quad (6)$$

with

$$\dot{Q}_{coll} = \eta_{coll} \cdot \dot{Q}_{sun} = \eta_{coll} \cdot A_r \cdot H_b \cdot b_{tracking} \quad (7)$$

Equation 6 can also be written as:

$$\frac{dU}{dt} = \dot{Q}_{coll} - \dot{Q}_{PT} - \dot{Q}_{VAP} - \dot{Q}_{SC} \quad (8)$$

where

$$\dot{Q}_{SC} = \dot{m}_{in} \cdot (h_s - h_{in}) \quad (9)$$

$$\dot{Q}_{PT} = (\dot{m}_{out} - \dot{m}_{in}) \cdot h_s \quad (10)$$

$$\dot{Q}_{VAP} = \dot{m}_{out} \cdot (h_{out} - h_s) \quad (11)$$

At steady state, the energy necessary for changing the thermo-physical conditions of the fluid from incoming sub-cooled liquid to saturated steam can be divided into three terms:

- \dot{Q}_{SC} is the heat supply for bringing the sub-cooled condensate coming from the user with a flow rate \dot{m}_{in} up to saturated liquid conditions.
- \dot{Q}_{PT} is the energy required to compensate for any inlet/outlet flow rate imbalance;
- \dot{Q}_{VAP} is the energy necessary for heating the required flow rate \dot{m}_{out} from saturated liquid to saturated steam conditions.

The heat transfer diagram (Figure 3) represents the processes \dot{Q}_{SC} and \dot{Q}_{VAP} ; i.e. heating of the sub-cooled condensate, and heating steam up to the required conditions (as described in Eq. 9-11). At steady state ($dU/dt = 0$), the external heat supply for these processes should come from the solar collector.

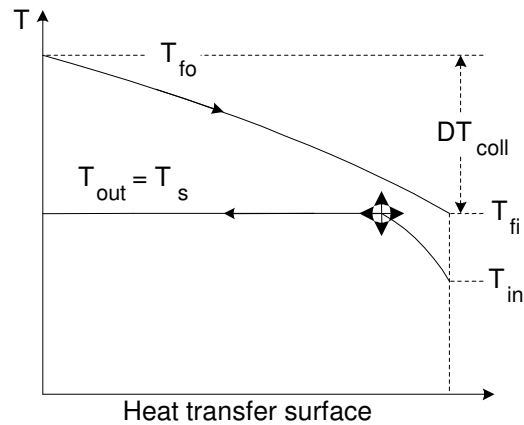


Figure 3: SA Heat Transfer Diagram.

The collector is operated with a minimum inlet temperature $T_{fi} = T_s$ (saturation temperature inside the SA), so that the temperature difference at the pinch point is always positive. In practice this corresponds to having a large heat transfer surface inside the SA.

In the simplest case, the collector is operated by modulating the flow rate in order to maintain a fixed value of DT_{coll} . The crossed arrows at the pinch point in Fig. 3 can be interpreted in the following way:

- the pinch point can move left or right (the right most position, i.e. no sub-cooled liquid, corresponds to $\dot{m}_{in} = 0$).
- the pinch point can move up and down according to the pressure inside the SA.

Whenever the solar collector heat flux \dot{Q}_{coll} is not sufficient to cover the heat demand, the pressure and temperature inside the SA drop. This leads to steam flashing and thus more process steam. Therefore, this system is self-regulating.

Starting from specified initial conditions (pressure/temperature, fill level), the dynamic behavior of the system is modeled for a specified set of time-dependent rules for \dot{m}_{out} and \dot{m}_{in} . In most industrial systems \dot{m}_{in} is kept approximately constant by using a condensate recovery tank (usually at atmospheric pressure). On the other hand, the mass flow rate \dot{m}_{out} depends on the heat demands. The energy balance (Eq. 1) gives the thermal power input from the collector. Should the solar collector not be able to provide enough heat, an external burner would be activated.

3. Sample Application

The reference data for the sample application (Table 1) were adapted from those originally available for a dairy, which uses heat – presently provided by two industrial oil boilers – to maintain a steam accumulator connected to a local plant distribution network. Heat is used for the pasteurization of milk and for the daily cleaning of equipment and working rooms.

The time histories of \dot{m}_{in} and \dot{m}_{out} over a reference day (in April) as well as the filling level of the SA are shown in Figure 4. The dynamic behavior of the pressure and temperature in the SA are presented in Figure 5, while Figure 6 shows the behavior of the different heat rates over the day: \dot{Q}_{coll} , \dot{Q}_{SC} , \dot{Q}_{PT} , and \dot{Q}_{VAP} .

4. Exergy Analysis

Once the mass and energy balances of the system have been calculated, it is possible to perform an exergy analysis in order to locate the main exergy destructions. The input exergy is approximately equivalent to the absorbed radiation coming from the sun (which is reasonable in this case as the equivalent sun temperature is much higher than that of the collector). Once the time histories of \dot{m}_{in} and \dot{m}_{out} are specified, the output exergy can be determined by the exergy difference of inlet and outlet of the SA. Consequently, the system exergy output during the day operation is specified and is not a matter of improvement.

Figure 7 shows the variation of the SA exergy over the day.

From the exergy balance of the system and of the collector, it is possible to calculate the system's exergy efficiencies. The input exergy is the exergy of radiation from the sun (\dot{E}_{SUN}) over the gross collector surface.

For the reference day, the exergy efficiencies are shown in Figure 8. A detailed analysis of the indirect buildup of the system exergy balance is summarized in Figure 9, representing the three system exergy destructions/losses:

- ExL_{collHD} is the exergy loss due to heat dissipation from the solar collector to the environment (Manfrida, 1985; Manfrida and Kawambwa, 1991)
- ExD_{collHT} is the exergy destruction due to the heat transfer from the sun to the solar collector (Manfrida, 1985; Manfrida and Kawambwa, 1991)

Table 1: Reference Data.

Variable	Symbol [unit]	Value
Initial pressure	p [bar]	5
Minimum pressure	p _{min} [bar]	2,5
Maximum pressure	p _{max} [bar]	7,5
SA volume	V [m ³]	16
Initial fill level	F	80%
Number of collectors	z	70 (61)
Collector size	L; b [m]	5; 1,5
Collector DT	DT _{coll} [°C]	80 (10)
Month of year		April
Condensate return T	T _i [°C]	80

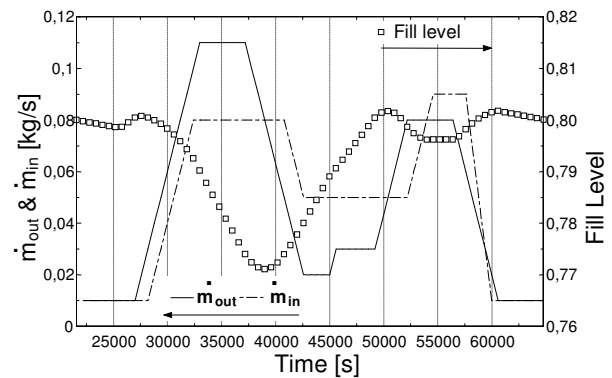


Figure 4. Time History of SA Inlet/Outlet Flow Rates and Filling Level.

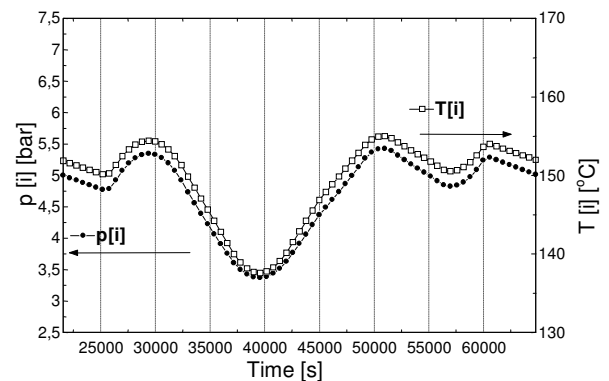


Figure 5: Time History of SA Pressure and Temperature.

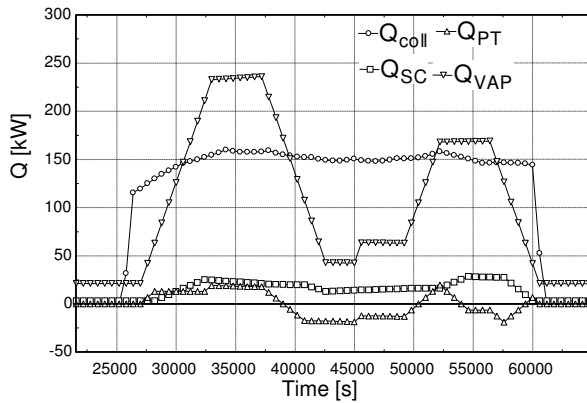


Figure 6: Calculated System Heat Rates.

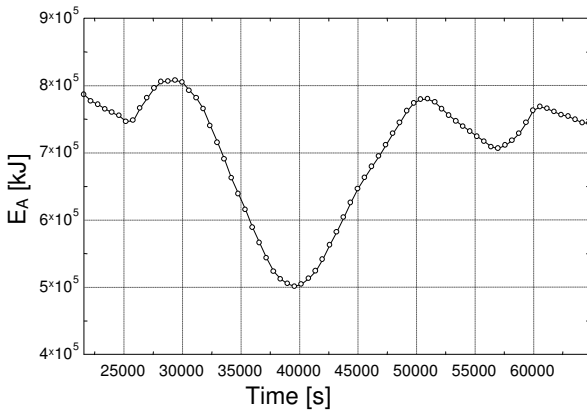


Figure 7: Calculated Steam Accumulator Exergy.

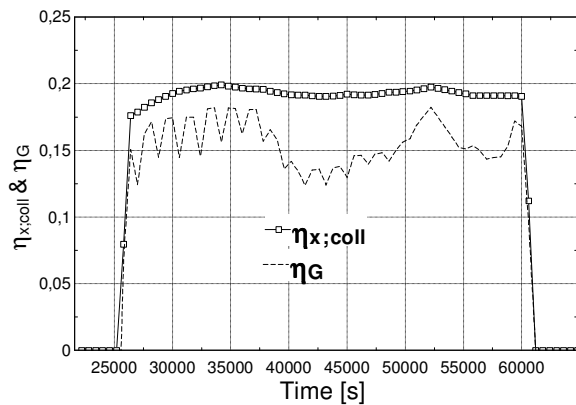


Figure 8: Calculated Exergy Efficiencies, ($DT_{coll}=80^{\circ}C$).

- $T_a DS_{irr}$ is the transient exergy destruction in the steam accumulator, resulting from the balance:

$$T_a DS_{irr} = -\frac{dE_A}{dt} - \dot{E}_{A,out} + \dot{E}_{A,in} + \dot{E}_{coll} \quad (12)$$

$$\dot{E}_{A,out} = \dot{m}_{out} \cdot e_{A,out} \quad , \quad \dot{E}_{A,in} = \dot{m}_{in} \cdot e_{A,in} \quad (13)$$

The second largest contribution to exergy destruction is the collector-absorber heat transfer (ExD_{collHT}), i.e. the exergy destruction due to the change in the temperature level of the usable energy (from the sun temperature to the average absorber temperature). In contrast, the exergy

destruction due to the transient operation of the SA (Eq. 12) is negligible, since the temperatures of the absorber fluid in the collector and SA are close to each other. In Figure 9 also the following exergy rates of the SA are presented: the transient variation of exergy dE_A/dt , the input exergy rate from the solar collector \dot{E}_{coll} , and the difference in exergy $\dot{E}_{A,out} - \dot{E}_{A,in}$ (outlet steam – inlet water).

Due to the transient operation of the SA, the global exergy efficiency is clearly smaller than the collector efficiency. The total daily exergy efficiency for the reference day is $\overline{\eta}_G = 0.150$ calculated as:

$$\overline{\eta}_G = \int \frac{dE + \dot{E}_{out} - \dot{E}_{in}}{\dot{E}_{SUN}} dt \quad (14)$$

The system performance can be improved if the collector temperature difference DT_{coll} is decreased. This becomes clear by comparing Figure 10, in which the system's exergy destructions and exergy rates are presented for a value of $DT_{coll} = 10^{\circ}C$, with Figure 9 ($DT_{coll} = 80^{\circ}C$). With this lower value of DT_{coll} , the daily heat demand can be satisfied with 61 collectors (compared to 70 collectors in the case of $DT_{coll} = 80^{\circ}C$).

Lowering the collector temperature difference DT_{coll} to $10^{\circ}C$ (Figure 11 for the time history of exergy efficiency), the daily-averaged global exergy efficiency increases to $\overline{\eta}_G = 0.173$ for the same reference day.

Figure 12 shows the behavior of the specific volumetric flow rate (per unit collector area) V_{sp} through the solar collector at varying DT_{coll} . By lowering the collector temperature difference, the specific mass flow rate increases. The volumetric flow rates reported in Figure 12 are consistent with data for similar applications (Kalogirou et al., 1997).

5. Conclusions

The relatively simple thermodynamic model provides useful help for sizing the solar field and the steam accumulator for a given industrial application using medium/high temperature solar heat. Once the time-dependent heat loads are given and the main operating conditions are specified (upper/lower pressure limits, collector parameters), it is easy to determine the required size of the steam accumulator and of the solar field. The exergy analysis shows that the largest exergy destructions take place in the solar collector, while the contribution of the steam accumulator is relatively small. The main parameter determining the system's exergetic efficiency is the collector temperature difference DT_{coll} , which is directly linked to the specific flow rate across the collector.

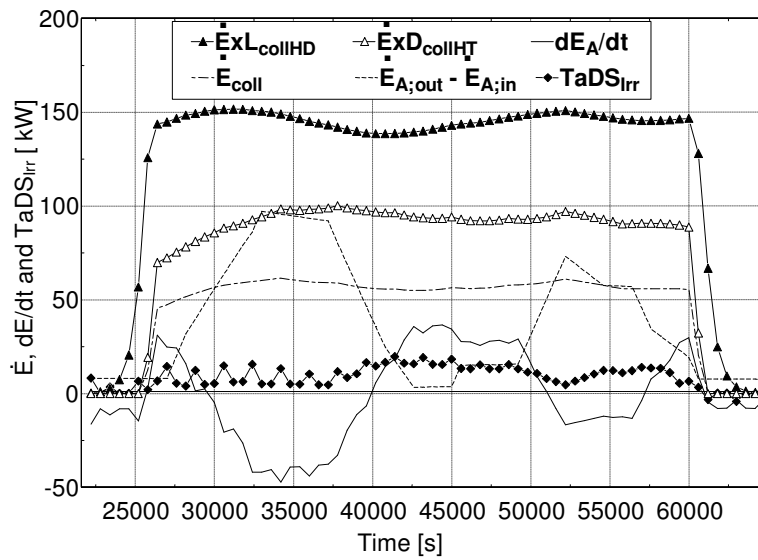


Figure 9: Calculated System Exergy Destructions/ Losses and Exergy Rates for the SA ($DT_{coll} = 80^\circ C$).

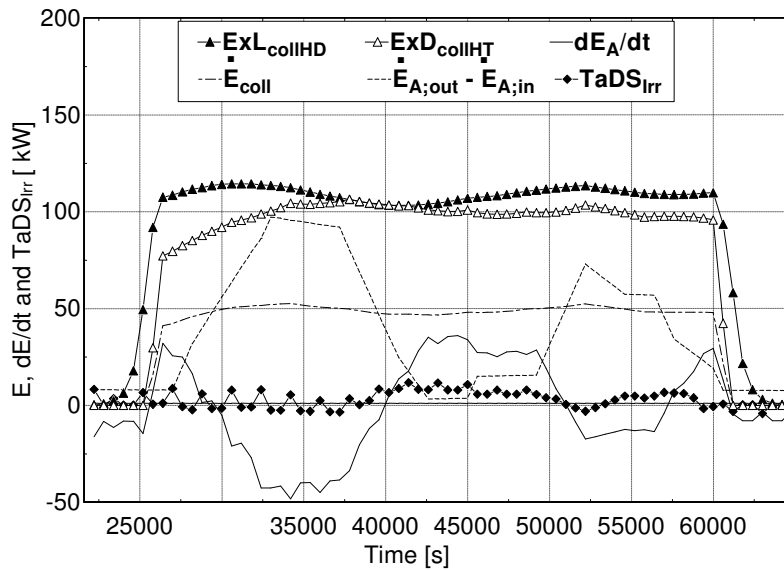


Figure 10: Calculated System Exergy Destructions and Exergy Rates for the SA ($DT_{coll} = 10^\circ C$).

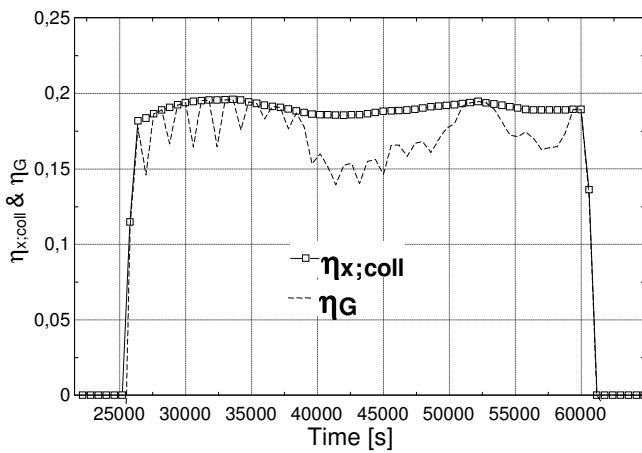


Figure 11: Calculated Exergy Efficiencies ($DT_{coll} = 10^\circ C$).

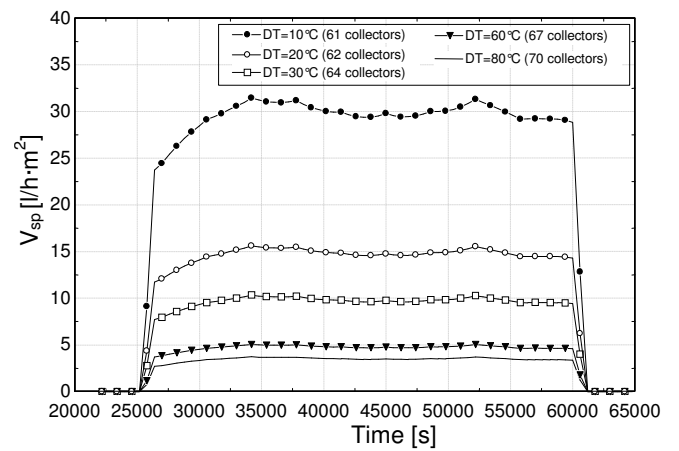


Figure 12: Volume Flow Rate per Unit of Collector Area.

Nomenclature

A	first constant for solar collector performance
A_r	solar collector aperture area, m ²
B	second constant for solar collector performance, kW/(m ² K)
b	collector width, m
C	third constant for solar collector performance, kW/(m ² K ²)
DT_{coll}	temperature difference through solar collector, °C
\dot{E}	Exergy, kW
ExD	Exergy destruction, kW
ExL	Exergy Loss, kW
F	steam accumulator fill level
h_{in}	enthalpy of \dot{m}_{in} , kJ/kg
h_{out}	enthalpy of \dot{m}_{out} , kJ/kg
h_s	enthalpy at saturated liquid condition in the Steam Accumulator, kJ/kg
$Hb_{horizontal}$	beam irradiance to horizontal surface, kW/m ²
$Hb_{tracking}$	beam irradiance to tracking surface by North-South axis, kW/m ²
I	solar irradiation, kW/m ²
L	Collector length, m
M	mass of water in the steam accumulator, kg
\dot{m}_{in}	mass flow rate entering in to the steam accumulator, kg/s
\dot{m}_{out}	mass flow rate exiting from the steam accumulator, kg/s
\dot{m}_{PT}	mass flow rate - phase transition inside the steam accumulator, kg/s
\dot{m}_{TV}	mass flow rate passing through solar collectors, kg/s
p_{max}	maximum pressure in the steam accumulator, bar
p_{min}	minimum pressure in the steam accumulator, bar
\dot{Q}_{coll}	heat rate to heat transfer fluid in the solar collector, kW
\dot{Q}_{PT}	heat rate to compensate for any inlet/outlet flow rate imbalance in steam accumulator, kW
\dot{Q}_{SC}	heat rate from subcooled to saturated liquid condition in steam accumulator, kW
\dot{Q}_{sun}	heat rate from sun to the solar collector, kW
\dot{Q}_{VAP}	heat rate from saturated liquid to saturated steam condition in steam accumulator, kW

SA	steam accumulator
T_a	ambient temperature, °C
T_i	condensate return temperature, °C
T_{fi}	solar collector inlet temperature, °C
T_{fo}	solar collector outlet temperature, °C
T_s	saturation temperature inside the steam accumulator, °C
U	internal energy, kJ
V	steam accumulator volume, m ³
V_{sp}	volume flow rate through solar collectors per unit of solar collector area, l/(h·m ²)
X	solar collector working condition parameter, m ² K/kW
z	number of collectors
δ	declination angle, °
θ	surface angle, °
θ_s	zenith angle, °
η_{Coll}	solar collector thermal efficiency
η_G	global system exergetic efficiency
η_{xColl}	solar collector exergetic efficiency
ω	hour angle, ° (0 at midday, negative at sunrise, positive at sunset)

Subscripts

A	steam accumulator
$Coll$	collector
$CollHD$	collector heat dissipation
$CollHT$	collector heat transfer
D	destruction
Irr	irreversibility (time-varying contribution)

References

- Camacho, E., Berenguel, F., Rubio, R., 1997, *Advanced Control of Solar Plants*, Springer Verlag, London.
- Duffie J, Beckham W., 2006, *Solar engineering of thermal processes*, John Wiley & Sons.
- Kalogirou S., Lloyd S., Ward J., 1997, "Modelling, optimisation and performance evaluation of a parabolic trough solar collector steam generation system", *Solar Energy*, Vol. 60, pp. 49-59.
- Manfrida, G., 1985, "The Choice of the Optimal Working Point for Solar Collectors", *Solar Energy*, Vol. 34, pp. 6-7
- Manfrida, G., Kawambwa, S., 1991, "Exergy control for a flat-plate Collector/Rankine Cycle Solar Power System", *ASME J. of Solar Energy Engineering*, Vol. 113, pp. 89-93.
- Mills, D., 2004, "Advances in solar thermal electricity technology", *Solar Energy*, Vol. 76, pp. 19-31
- Winter, C.J., et al., 1991, *Solar Power Plants* Springer, New York.